J. Micromech. Microeng. **20** (2010) 085007 (7pp) doi:10.1088/0960-1317/20/8/085007

Scanning grating based in-plane movement sensing

Hongbin Yu[1], **Guangya Zhou**[1], **Sujeet Kumar Sinha**[2] **and Fook Siong Chau**[1]

[1] Micro/Nano Systems Initiative Technology, Department of Mechanical Engineering, National University of Singapore, Singapore 117576
[2] Material Laboratory, Department of Mechanical Engineering, National University of Singapore, Singapore 117576

E-mail: mpezgy@nus.edu.sg

Received 15 May 2010, in final form 5 June 2010
Published 2 July 2010
Online at stacks.iop.org/JMM/20/085007

Abstract
A novel method for detecting the in-plane movement of MEMS devices has been presented, in which a scanning grating structure has been adopted. One end of the grating is directly connected to the movable platform under test, while the other end is fixed to a substrate, both by a suspending beam. Due to this structure design, any in-plane movement of the platform will be finally translated into grating rotation. When a laser beam is incident onto the grating, the direction of diffracted light as well as its spot position on a photosensitive device (PSD) will be changed accordingly due to the grating rotation. From the output of the PSD, the movement amplitude can be finally determined. With this novel sensing mechanism, not only static and dynamic movements, but also the transient structure response have been experimentally demonstrated.

(Some figures in this article are in colour only in the electronic version)

Introduction

Movement sensing is a very important topic in metrology. In some cases, the measurement of structural movement induced by the exterior environment can be adopted to acquire particular information [1]. For example, the resultant translation/rotation of the proof mass has been widely used for acceleration sensing (e.g. accelerometer and gyroscope), and in many cases, the obtained data will be further used as a feedback controlling signal for realizing closed-loop operation, which can find wide applications in civilian and military areas such as servo-control of a fabrication machine and automotive robot, scanning display, entertainment electronics, target tracking and navigation, etc. At the same time, the resultant deflection of a cantilever beam with its tip interacting with a surface can be used to characterize the surface quality (e.g. roughness), which is the key working theory of atomic force microscopy (AFM)—one of the most important and commonly used facilities for occasions concerning much about surface (e.g. optics and microelectronics industries) [2].

With the flourishing development of micro/nano-electro-mechanical systems (M/NEMS), the involved feature dimension further extends to micro- and nano-scale. Therefore, suitable movement sensing (especially non-contact configuration) with high resolution, which demonstrates good compatibility with M/NEMS, has attracted more and more research interest. Till now, many methods have been successfully reported. A piezoresistive-type sensing mechanism is one of the most widely adopted methods, which has already been successfully used in a macro area [3, 4]. It works based on the change in a resistor caused by deflection. The measuring sensitivity is directly determined by the piezoresistive coefficient of material constituting the resistor. The larger the coefficient, the smaller the movement that can be discerned. As a result, in real applications some impurities, such as B and P, are commonly doped into silicon via diffusion or implanting to increase its piezoresistive coefficient [5]. Although this treatment is compatible with the mainstream fabrication process, the additional involved steps will definitely complicate the fabrication and increase its period and failure probability. Meanwhile, the effect of environmental

temperature on this coefficient as well as the final measurement accuracy is also a problem. Another commonly reported sensing method is based on a capacitor configuration. The capacitor consists of two or two sets of parallel plates. One is fixed to a substrate and the movable structure under test itself constitutes the other one. Any structural movement will change the distance or the overlapping area between these two plates, thus varying the capacitance value. Through reading out this variation, the movement information can be obtained [6–8]. The capacitor structure is very simple for fabrication and can be easily integrated into a device structure without affecting its performance so much. Since all the signals involved are of electrical type, however, sophisticated wiring layout, signal sampling and processing circuits are dispensable, and at the same time, interference coming from exterior environment, such as electromagnetic interference and parasitic effect, should also be carefully eliminated.

Besides the above-mentioned electrical signal-based sensing configurations, optical measuring methods have also been widely developed. The working theory of most optical measuring methods is based on laser interference [9]. For example, the configurations—Michelson and Mirau interferometer integrated into the optical system of microscopy—have been widely adopted in a commercialized profiler (Zygo and Wyko). This type of method is especially suitable for static measurement and can easily achieve a sub-nanometer measuring resolution in the vertical direction (namely out-plane), whereas the resolution for in-plane movement is mainly determined by the optical system resolution. In order to achieve the capability for measuring dynamic movement, strobed illumination has been introduced into interferometry [10, 11], such as the DMEMS Dynamic MEMS Measurement option (Veeco, USA). Although moving MEMS devices have been successfully characterized, considering the fact that the measurement for movement in one period usually requires the object under test to be moved several periods, this method is appropriate for the case exhibiting good moving repeatability. When treating cases involving time-dependent and non-reversible movement, such as friction and wear test, the task of real-time movement monitoring is beyond the capability of this method. Another commonly used optical measuring method is laser Doppler technology [12, 13]. By combining the frequency modulation effect (Doppler effect) induced by movement with interference, both velocity and displacement can be simultaneously measured. In order to obtain high resolution and real-time measuring capability, however, there is a high requirement on the following signal processing unit.

In this paper, a novel in-plane movement sensing method, which demonstrates easy operation, high versatility and concise configuration, has been presented. It works based on movement-induced laser scanning via a rotational grating structure. The laser is finally incident onto a photosensitive device (PSD) and its spot position is directly relevant to the movement under test. As a result, from the output of the PSD, the movement information, including static, dynamic and transient movement, can be easily obtained with this proposed method in real time.

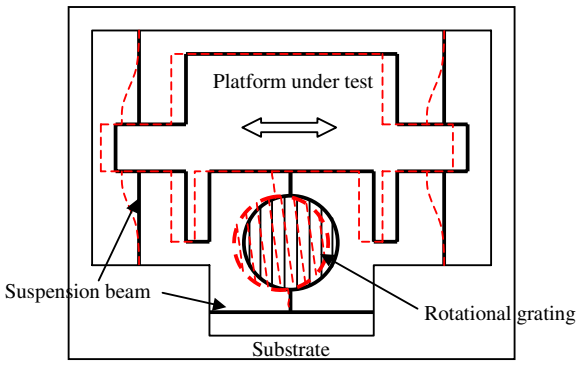

Figure 1. Schematic of the in-plane movement sensing structure.

Structure design

The basic idea of structure design for the currently proposed movement sensing mechanism is to translate the movement into laser scanning, which is similar to the detection mechanism adopted in some well-known AFM. In the current design, this translation function is realized via an in-plane rotational grating structure, which was first developed by Zhou *et al* for high speed scanning purposes [14–17]. One end of the grating is directly connected to the movable platform, which is suspended by two sets of folded beams and actuated with electrostatic comb-drive actuators, while the other end is fixed to a substrate, both using a suspension beam as schematically shown in figure 1. During measurement, a laser beam is made incident onto the grating. It is then diffracted into several orders with their angles θ_m determined by [18]

$$\sin(\theta_m) = m\lambda/d + \sin\alpha, \tag{1}$$

where m is the diffraction order, d is the grating period, λ and α are the wavelength and incidence angle of the laser beam, respectively.

When the grating is rotated, the direction of the diffracted beam will be changed accordingly. If the PSD is used to collect the diffraction, with the direction variation of diffraction, its spot position on the PSD as well as the PSD output will also be changed. Figure 2 shows the schematic of the grating scanning-based sensing mechanism.

The laser is normally incident ($\alpha = 0$) onto the grating and the PSD is arranged at a position parallel to the 'YOZ' plane and the distance between them is defined by 'a'. When the grating is rotated by ϕ, the resultant laser spot movement on the PSD can be described by

$$m_Y = a \cdot \tan(\phi) \tag{2}$$

$$m_Z = \frac{a}{\tan(\theta_m)} \cdot \left(\frac{1}{\cos(\phi)} - 1\right), \tag{3}$$

where m_Y and m_Z are the spot movement along the Y and Z axes, respectively.

In the current experiment, the grating period is chosen to be 4 μm (considering the compatibility to the fabrication

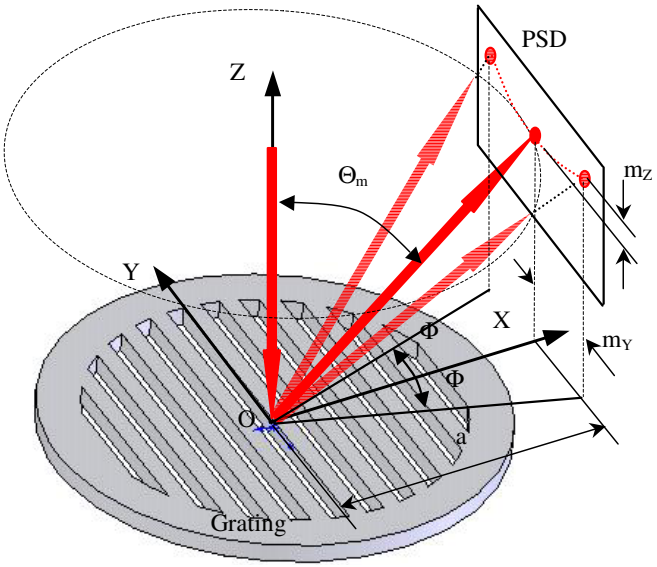

Figure 2. Schematic of the grating scanning-based sensing mechanism.

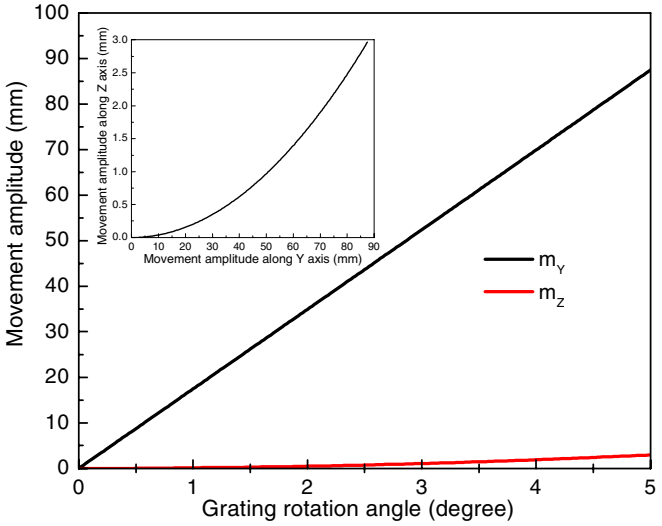

Figure 3. Spot movements on the PSD as a function of the grating rotation angle. Inset is the spot moving orbit on the PSD.

rule) and the PSD is arranged at a position 1 m distant. At the same time, the fifth-order diffraction of the normally incident red laser (632.8 nm wavelength) is used as a sensing beam. By substituting these values into equations (1)–(3), the spot movement with respect to the grating rotation angle can be obtained as shown in figure 3.

It is obvious that within 5° grating rotation angle, the spot movement along the *Y* axis increases linearly with increasing rotation angle (variation slope is 17.493 mm/deg) and its movement amplitude is much larger than that along the *Z* axis. Since the output of the PSD is proportional to the movement amplitude, larger movement amplitude under certain grating rotation results in larger PSD output, demonstrating higher sensing resolution.

The design of a grating suspension structure as well as the simulation results from grating operation using ANSYS is given in figure 4. The connection between the grating and

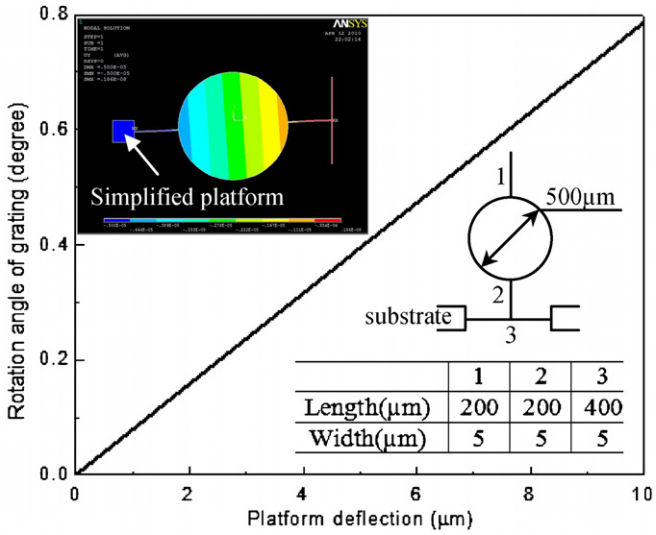

Figure 4. Simulation result of the grating rotation angle as a function of platform deflection. *The structural thickness is 25 μm.

movable platform is a straight beam, while that to the substrate is designed to be T shape, in which the transverse beam (connecting directly to substrate) acts as a stress releasing beam, making the response of the grating more linear within the measuring range (detailed analysis can be found in [19]).

From figure 4 it can be seen that the relationship between the grating rotation angle and platform lateral deflection demonstrates good linearity within the concerned 10 μm moving amplitude with a slope of 0.079 deg μm^{-1}. By combining the results shown in figure 3, when using the spot movement along the *Y* axis, namely m_Y, as the sensing signal, it can be seen that 1 μm platform movement will eventually cause 1.382 mm spot movement (m_Y) (1 μm $\times$ 0.079 $^\circ$ μm^{-1} $\times$ 17.493 mm/deg = 1.382 mm), thus demonstrating 1382 deflection magnification. As a result, it can be foreseen that not only good linear response, but also higher resolution can be achieved in the proposed sensing mechanism. At the same time, since the spot movement is also proportional to the PSD position (equation (2)), it is very flexible to adjust the final performance with respect to different applications.

Device fabrication

The proposed device is fabricated via a standard commercial process flow 'SOIMUMPs' provided by MEMSCAP Inc. The schematic process flow is shown in figure 5. The fabrication begins with a double side polished SOI wafer; the thicknesses of the device layer, buried oxide and substrate are 25 μm, 1 μm and 400 μm, respectively. Then the first lithography step followed by first deep-RIE is used to fabricate the desired structure into the device layer. After that, the residual photoresist layer is removed away. Subsequently, the second lithography and deep-RIE steps are performed in sequence on the backside, namely substrate side, to make an opening in the substrate right under the structure region. By removing the photoresist and the exposed buried oxide, all the movable

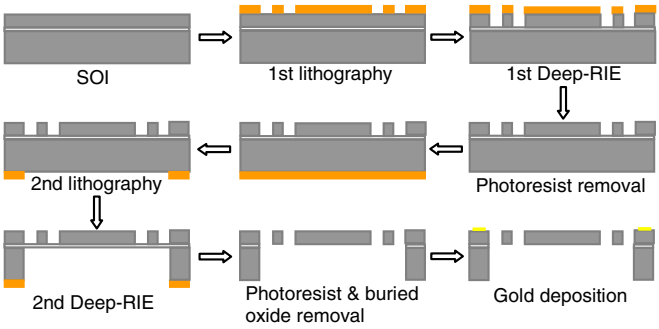

Figure 5. Fabrication process flow.

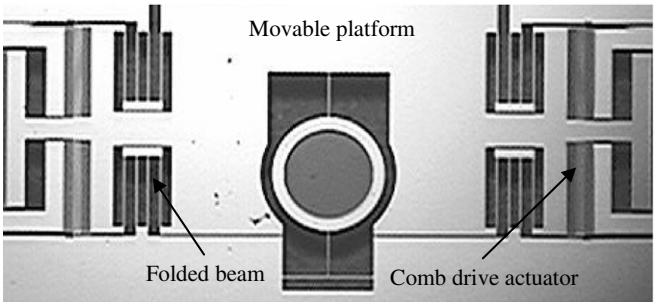

(*a*)

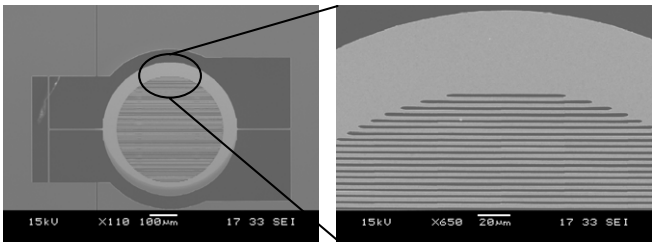

(*b*)

Figure 6. Fabrication results. (*a*) Microscopic picture of the whole device, (*b*) SEM of the grating sensing structure.

components can be released. Finally, a gold pad layer is deposited via e-beam evaporation. Figure 6(*a*) shows the microscopy picture of the whole device, including the movable platform and the grating sensing structure, while the SEM of the grating structure is given in figure 6(*b*).

Experimental results

In order to demonstrate in-plane moving sensing capability associated with the currently proposed method, three types of movements have been characterized, including static, dynamic and transient statuses. During experiment, S1880 (Hamamatsu, Japan) 2D PSD, with 1 mm V^{-1} linear output and 1.5 μm position resolution, is used.

Static status

In this measurement, several different dc voltage values are applied to comb-drive actuators, and the resultant PSD output is recorded, respectively. Combining the response of the PSD output with respect to spot movement on it (1 mm V^{-1}), the individual platform deflection can be calculated.

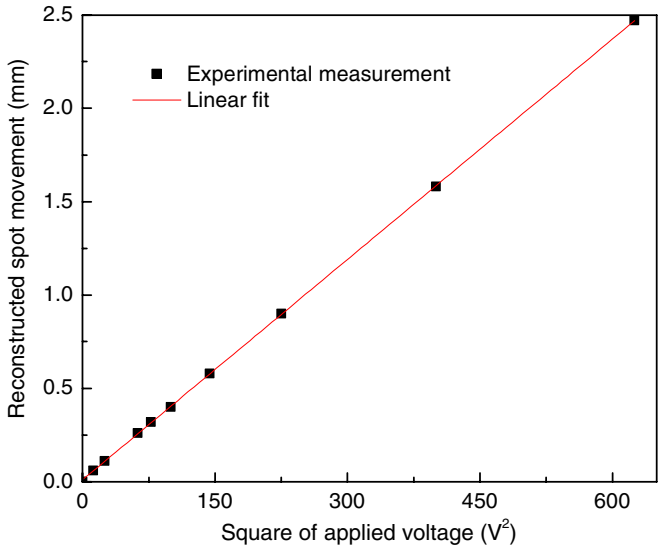

Figure 7. Reconstructed light spot movement as a function of the square of the applied voltage obtained from the experiment.

From theoretical analysis, it is well known that with respect to the comb-drive actuator, the generated electrostatic actuation force is proportional to the square of the voltage (V^2) applied. As a result, the resultant deflection should also exhibit linear variation with V^2 within the elastic region. Considering the linear relationship between the deflection and the resultant grating rotation (see figure 4) as well as the spot movement along the Y direction in the PSD plane (see figure 3), the PSD output should also demonstrate linear variation with V^2.

From the experimental results shown in figure 7, it can be seen that the reconstructed spot movement from the PSD output increases linearly from the original position to nearly 2.5 mm with the square of the applied voltage increasing from 0 to 625. After performing a linear fit to these data, the variation slope is calculated to be 0.003 94 mm V^{-2}. In order to characterize the sensing resolution of the proposed method, the deflections of the platform at different applied voltages have also been directly measured using a commercial profiler under 50× magnification (Zygo, USA), as shown in figure 8.

Similarly, a good linear relationship between the deflection and V^2 can also be found. However, the variation slope is now changed to 0.003 17 μm V^{-2}. As a result, it can be concluded that with the current sensing mechanism the platform movement can be finally translated into spot movement on the PSD with 1243 (0.003 94 (mm V^{-2})/0.003 17 (μm V^{-2})) magnification. Considering 1.5 μm position resolution of the PSD, the theoretical movement resolution provided by the current grating-based sensing mechanism can reach 1.2 nm.

Dynamic status

Besides static movement, in some cases, the device will be actuated to work under continuous status, such as a MEMS mechanical resonator, micro mirror scanner, etc. As a result, dynamic movement sensing capability should also

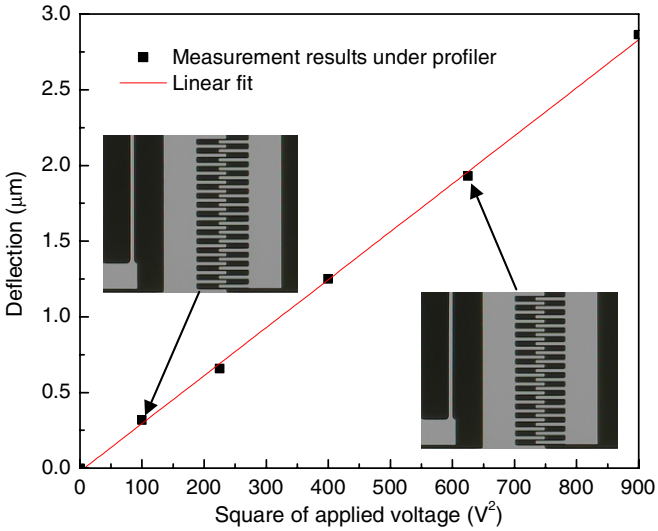

Figure 8. Measured platform deflections as a function of the square of the applied voltage using a Zygo profiler. (Insets are pictures of the comb-drive fingers under different statuses, in which the left fingers are fixed, while the right ones are connected to a movable platform.)

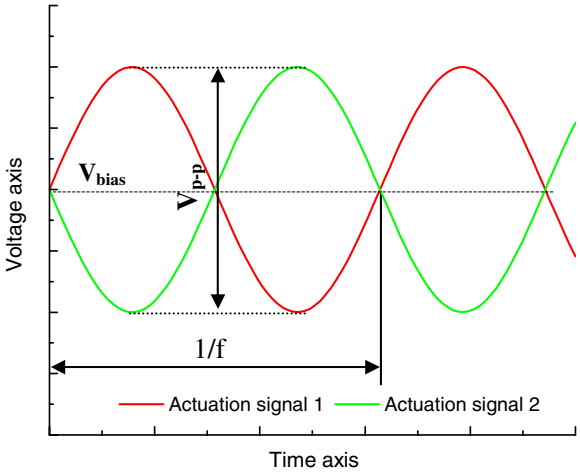

Figure 9. Schematic of the applied actuation signal used in the dynamic movement sensing experiment.

play an important role. During this experiment, two ac sinusoidal actuation signals with the same frequency (f), dc bias (V_{bias}) and V_{p-p} amplitude but a 180° phase difference as schematically shown in figure 9 are usually applied to two sets of comb-drive actuators arranged in opposite directions, respectively. From theoretical analysis, the resultant actuation force $F(t)$ as well as the time-dependent deflection $d(t)$ can be given by

$$F(t) \propto \left[V_{\text{bias}} + \frac{V_{p-p}}{2} \cdot \sin(2\pi f t)\right]^2 - \left[V_{\text{bias}} - \frac{V_{p-p}}{2} \cdot \sin(2\pi f t)\right]^2$$

$$d(t) \propto F(t) \Rightarrow d(t) \propto V_{\text{bias}} \cdot V_{p-p} \sin(2\pi f t). \quad (4)$$

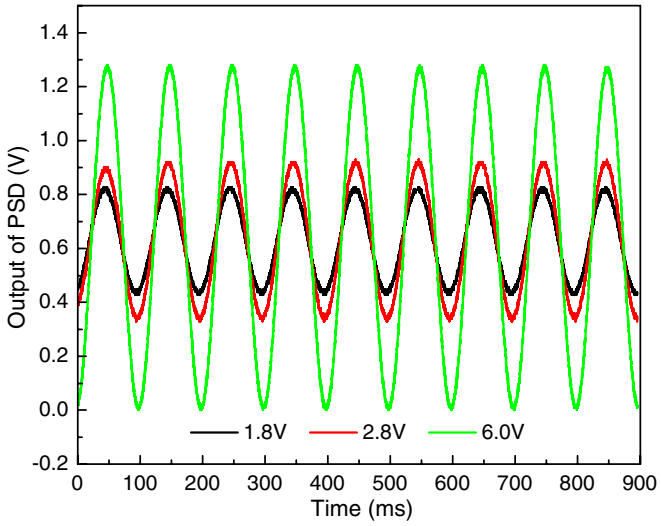

Figure 10. PSD output of dynamic movement sensing.

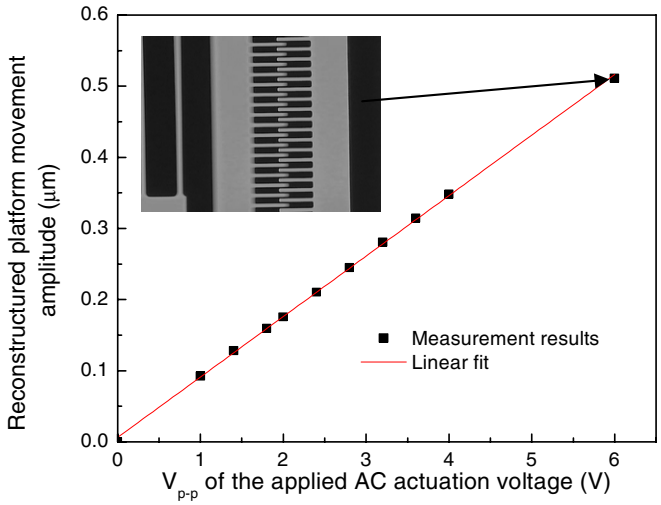

Figure 11. Reconstructed platform movement amplitude as a function of V_{p-p} of the applied ac actuation voltage.

It is obvious that under this working condition, the final deflection is proportional to the V_{p-p} amplitude of the applied signal.

In the current experiment, the ac sinusoidal actuation signal with 10 Hz frequency, 5 V dc bias and several different V_{p-p} amplitudes has been adopted. All the outputs of the PSD are directly captured with an oscilloscope and three of them are selectively shown in figure 10. By considering the movement magnification effect as mentioned above, the real movement amplitude can be finally reconstructed as provided in figure 11. At the same time, the image of comb-drive fingers working under this status is also provided as inset. The blurred edge is mainly caused by the dynamic movement.

From the PSD output signal, the sinusoidal vibration movement of the platform with fixed 10 Hz frequency, the same as that of the actuation signal, can be revealed the amplitude of which increases linearly with the applied voltage amplitude, agreeing well with theoretical analysis (equation (4)).

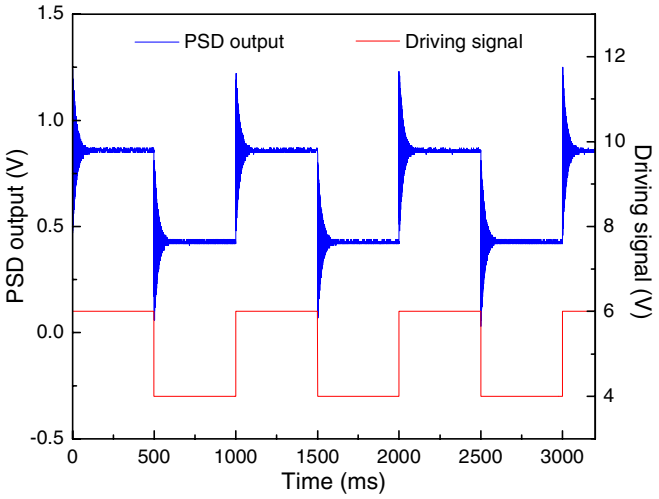

Figure 12. PSD output at a square wave actuation signal.

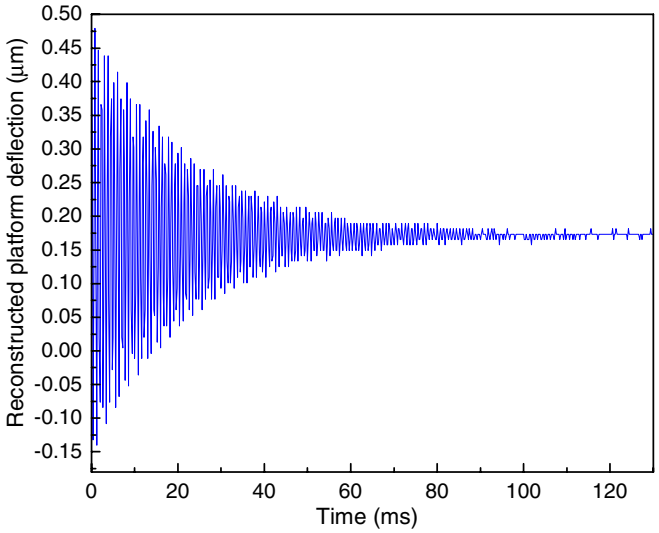

Figure 13. Reconstructed platform transient deflections.

Transient status

In some applications, the transient response of the device will directly determine the system working bandwidth. For example, in the RF application area, the response speed of MEMS switch is one of the most important criteria. It is well known that when a step stimulus is applied, the corresponding response of the system can be described by

$$d(t) = \frac{F}{k}\left[1 - \mathrm{e}^{-\zeta p_n t}\left(\cos p_d t + \frac{\zeta p_n}{p_d}\sin p_d t\right)\right]$$
$$p_n = \sqrt{k/m}, \qquad \zeta = C/(2p_n m), \qquad p_d = p_n\sqrt{1-\zeta^2}, \tag{5}$$

where m and k are the mass of the whole system and the equivalent spring constant of the supporting structure, respectively. C is the coefficient of air damping. p_n and p_d are angular frequency of the system operating with and without the damping effect, respectively.

In this experiment, a 1 Hz square wave signal with 2 V V_{p-p} amplitude and 5 V DC bias is adopted. Figure 12 shows the obtained PSD output under this working condition. From the reconstructed response of the platform deflection as shown in figure 13, a typical response characteristic associated with an underdamped second-order system, as described by equation (5), can be found, which is mainly caused by the air damping effect as widely reported in the operation of MEMS devices [20, 21]. Through standard analysis, it can be seen that the rise time of the current system under test is around 208 μs and overshoot and settling time are 78.6% and 80 ms, respectively. At the same time, the period of deflection is 0.8 ms; therefore, the damped natural frequency of the current system can be deduced to be 1250 Hz.

Conclusion

In this paper, a novel in-plane movement sensing mechanism has been presented. The key idea is based on movement conversion, in which the in-plane movement will be translated into grating rotation. During measurement, a laser beam is directly incident onto the grating and one order of the diffractions is then received by the PSD, acting as a sensing signal. Once the grating rotation has occurred, the transmission angle of the diffraction will also be changed accordingly, therefore causing spot movement on the PSD. By reading the resultant PSD output, information about in-plane movement can be finally obtained. Due to the proposed structure design, smaller in-plane movement will be translated into enlarged spot movement. As a result, despite the relatively simple system configuration and sampling process, high measurement resolution (nearly 1.8 nm) can be achieved from the experiment result of static movement measurement. At the same time, the dynamic in-plane movements of the platform as well as its transient response to step stimulus have been successfully characterized, demonstrating high versatility of this measuring method.

Acknowledgments

Financial support by the National Research Foundation (NRF), Singapore, under award no NRF-CRP 2-2007-04 and the Ministry of Education Singapore AcRF Tier 1 funding under grant R-265-000-306-112 are gratefully acknowledged.

References

[1] Placko D 2007 *Fundamentals of Instrumentation and Measurement* (New York: Wiley)
[2] Whitehouse D J 2003 *Handbook of Surface and Nanometrology* (Bristol: IOP)
[3] Fiorillo A S 1997 A piezoresistive tactile sensor *IEEE Trans. Instrum. Meas.* **46** 15–7
[4] Peng C T, Lin J C, Lin C T and Chiang K N 2005 Performance and package effect of a novel piezoresistive pressure sensor fabricated by front-side etching technology *Sensors Actuators* A **119** 28–37
[5] Madou M J 1997 *Fundamentals of Microfabrication* (New York: CRC)
[6] Lee J, Huang X and Chu P B 2009 Nanoprecision MEMS capacitive sensor for linear and rotational positioning *J. Microelectromech. Syst.* **18** 660–70

[7] Baxter L K 1997 *Capacitive Sensors: Design and Applications* (Piscataway, NJ: IEEE Press)
[8] Horenstein M N, Perreault J A and Bifano T G 2000 Differential capacitive position sensor for planar MEMS structures with vertical motion *Sensors Actuators* A **80** 53–61
[9] Malacora D, Servín M and Malacora Z 2005 *Interferogram Analysis for Optical Testing* (Broken Sound Parkway, NW: CRC Press)
[10] Novak E, Wan D S, Unruh P and Schmit J 2003 Dynamic MEMS measurement using a strobed interferometric system with combined coherence sensing and phase information *Proc. Int. Conf. on MEMS, NANO and Smart Systems* pp 285–8
[11] Guo T, Chang H, Chen J, Fu X and Hu X 2009 Micro-motion analyzer used for dynamic MEMS characterization *Opt. Lasers Eng.* **47** 512–7
[12] Kim M G, Jo K, Kwon H S, Jang W, Park Y and Lee J H 2009 Fiber-optic laser Doppler vibrometer to dynamically measure MEMS actuator with in-plane motion *J. Microelectromech. Syst.* **18** 1365–70
[13] Zhang G X, Zhong Y, Hong X and Leng C L 2009 Microelectromechanical systems motion measurement and modal analysis based on Doppler interferometry *J. Vac. Sci. Technol.* B **27** 1251–5
[14] Zhou G and Chau F S 2006 Micromachined vibratory diffraction grating scanner for multiwavelength collinear laser scanning *J. Microelectromech. Syst.* **15** 1777–88
[15] Zhou G, Cheo K K L, Du Y, Chau F S, Feng H H and Zhang Q X 2009 Hyperspectral imaging using a microelectrical-mechanical-systems-based in-plane vibratory grating scanner with a single photodetector *Opt. Lett.* **34** 764–6
[16] Zhou G, Logeeswaran V J, Chau F S and Tay F E H 2004 Micromachined in-plane vibrating diffraction grating laser scanner *IEEE Photon. Technol. Lett.* **16** 2293–5
[17] Zhou G, Logeeswaran V J and Chau F S 2009 Optical scanning using vibratory diffraction gratings *US Patent* 7542188
[18] Woo D K, Hane K and Lee S K 2008 High order diffraction grating using V-shaped groove with refractive and reflective surfaces *Opt. Express.* **16** 21004–11
[19] Du Y, Zhou G, Cheo K L, Zhang Q X, Feng H H and Chau F S 2009 A 2-DOF circular-resonator-driven in-plane vibratory grating laser scanner *J. Microelectromech. Syst.* **18** 892–904
[20] Yang Y J J and Yen P C 2005 An efficient macromodeling methodology for lateral air damping effects *J. Microelectromech. Syst.* **14** 812–28
[21] De S K and Aluru N R 2006 Coupling of hierarchical fluid models with electrostatic and mechanical models for the dynamic analysis of MEMS *J. Micromech. Microeng.* **16** 1705–19